Mobility of Green Fluorescent Protein in Hydrogel-Based Drug-Delivery Systems Studied by Anisotropy and Fluorescence Recovery After Photobleaching

Andreas Bertz,† Jan-Eric Ehlers,† Stefanie Wöhl-Bruhn, Heike Bunjes, Karl-Heinz Gericke, Henning Menzel*

Modified hydroxyethyl starch is photo-crosslinked in the presence of a green fluorescent protein (GFP) (mTagGFP) to obtain loaded hydrogels as model for a drug-delivery system. An important factor for the protein release is the crosslinking density since a dense network should lead to hindered diffusion. To obtain information on the rotational and translational diffusion of GFP in the hydrogel, mTagGFP is analyzed by fluorescence anisotropy and fluorescence recovery after photo-bleaching experiments using two-photon excitation. The mTagGFP shows a viscosity-retarded rotational and strongly hindered translational diffusion, depending on the polymer concentration. A comparison of anisotropy studies with mTagGFP-loaded microparticles and hydrogel disks allows the polymer concentration to be determined for the microparticles, which has been previously unknown.

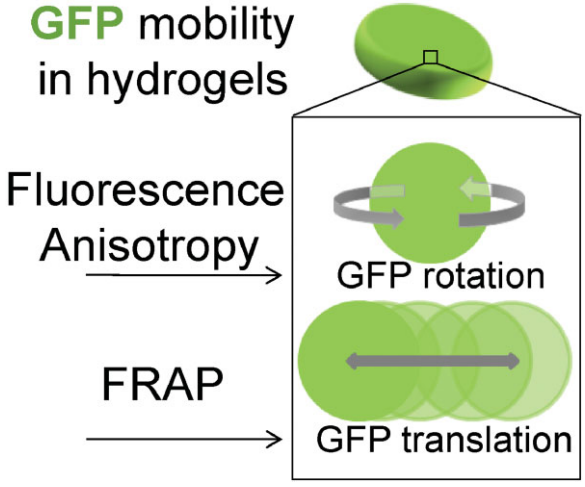

1. Introduction

Hydrogels and hydrogel microparticles can be loaded with highly specific therapeutic peptides or proteins like, for example, antibodies.[1,2] These increasingly important biopharmaceuticals can be used to treat various diseases like cancer and inflammatory disorders but they are often quickly degraded under physiological conditions.[3] Usually, frequent injections of the proteins have to be administered to the patient to retain the therapeutic concentration.[4] To avoid inconvenient continuous injections of high amounts of protein, to minimize drug dispersion in the body and to prevent protein degradation,

A. Bertz, Prof. H. Menzel
Technische Universität Braunschweig, Institute of Technical Chemistry, Hans-Sommer-Str. 10, 38106 Braunschweig, Germany
E-mail: h.menzel@tu-braunschweig.de
Dr. J.-E. Ehlers, Prof. K.-H. Gericke
Technische Universität Braunschweig, Institute of Physical Chemistry, Hans-Sommer-Str. 10, 38106 Braunschweig, Germany
S. Wöhl-Bruhn, Prof. H. Bunjes
Technische Universität Braunschweig, Institute of Pharmaceutical Technology, Mendelssohnstr.1, 38106 Braunschweig, Germany

† These authors contributed equally to this work.

DOI: 10.1002/mabi.201200325

drug-delivery systems (DDS) have to be developed. As carriers they can protect incorporated drugs from degradation and release them locally over a long period of time. Hydrogels are promising DDS for this kind of application because they provide an optimal protein environment and high loading capacities.[2,5]

The actual protein release depends on many factors, like the gel structure, the degradation properties, and the acceptor medium.[6–9] Release studies are a widely used tool for analysis, but they can be very time consuming, require significant quantities of material, and are challenging, in particular when they have to be carried out to evaluate long-term delivery systems. The availability of faster analytical methods for gathering information about the mobility of incorporated substances in DDS could accelerate the development of such systems. Therefore, we tested two two-photon excitation fluorescence microscopic techniques for their ability to characterize the mobility of proteins in different hydrogel systems. The hydrogels were based on hydroxyethyl starch (HES) modified with poly(ethylene glycol) methacrylate (HES-P(EG)$_n$MA; $n = 6$ or 10) or methacrylate (HES-MA), a recently developed crosslinkable HES derivative.[10] Green fluorescent protein (GFP) was incorporated as model substance.

Fluorescence microscopy is an established and indispensable tool for investigations in medicine and cell biology. A vast number of fluorescent molecules are available for probing the microenvironment of these molecules which can be used for investigation of cell metabolism.[11–14] Besides its application in biology, fluorescence microscopy can also be used for investigating polymeric systems like hydrogels. Two-photon excitation fluorescence microscopy is similar to the widely used (one-photon) confocal laser scanning microscopy (CLSM).[15] Using a two-photon microscope equipped with a near-infrared (NIR) femtosecond-pulse laser has several advantages over one-photon fluorescence excitation. Two-photon excitation has an intrinsic three dimensional (3D)-resolution and allows straightforward 3D-imaging of the samples.[16,17] As a consequence of this intrinsic 3D-resolution, photo-damage of sensitive proteins is restricted to the currently imaged focal plane. Using NIR light enables high sampling depths which is important to study the homogeneity of the investigated samples. Furthermore, less scattering is observed when NIR light is used for fluorescence excitation instead of UV or blue light. The combination of femtosecond pulses and megahertz repetition rates together with an appropriate detection setup allow an observation of time-resolved fluorescence on a timescale of molecular dynamics.[18] By investigation of the time-resolved fluorescence anisotropy information about the rotational diffusion behavior of gel-incorporated molecules as for instance GFP can be obtained.[19] Fluorescence anisotropy experiments hence permit probing the molecular interaction between the sensor protein and a hydrogel.[20] The translational diffusion behavior can be examined using fluorescence recovery after photobleaching (FRAP),[21] a well-established analysis method that has already been applied for the investigation of hydrogel-based DDS.[22,23] For this method a small volume within the sample is bleached with high-power laser irradiation and subsequently imaged with the attenuated laser beam, as the initial intensity is restored due to diffusion of unbleached fluorescent molecules into the bleaching volume. Since two-photon excitation is intrinsically restricted to the diffraction limited focal volume, the bleaching is also limited to approximately the same volume. This allows the observation of real 3D-diffusion without any experimental constraints.[24,25] In addition, pulsed multiphoton excitation facilitates higher photobleaching depths due to quadratic power dependence.

In this study, GFP was used as reporter molecule for all of the fluorescence anisotropy and FRAP experiments because it has some distinct advantages over other types of fluorescent molecules. Since it is a protein, the interactions with the polymer network should be similar to those of biopharmaceuticals. In addition, the size of GFP (26 kDa) is in the same range of order as that of antibody fragments. Furthermore, the chromophore of GFP has a clear-defined binding situation and environment and is tightly bound inside the β-barrel.[26,27] Local motions and a strong influence of the solvent are severe problems associated with fluorophore-labeled proteins.[28,29] These problems are circumvented using GFP.

The hydrogels with incorporated GFP were prepared by dissolving the prepolymer in water and adding GFP before photo-crosslinking. The efficiency of the photo-crosslinking can be influenced by variation in irradiation time, irradiation wavelength and type of initiator.[30,31] Photo-polymerization is also suited for crosslinking of emulsified polymer solutions to obtain microparticles.[32] The mobility of GFP within hydrogels and hydrogel microparticles was evaluated by the two fluorescence methods and correlated with the parameters applied in the crosslinking process and the resulting crosslink density as determined by swelling measurements.

2. Experimental Section

2.1. Materials

1,1′-Carbonyldiimidazole (CDI) (≥90%), 4-dimethylaminopyridine (DMAP) (≥98%), tetrahydrofuran (THF), glycidyl methacrylate (GMA) (97%) and poly(ethylene glycol) methacrylate (P(EG)$_n$MA) ($n = 6$: $\overline{M}_n = 360\ g\ mol^{-1}$, $n = 10$: $\overline{M}_n = 526\ g\ mol^{-1}$), dimethyl phenylphosphonite (97%), 2,4,6-trimethylbenzoylchloride (97%), lithium bromide (≥99%), and 2-butanone (≥99.0%) were purchased

from Sigma–Aldrich (Germany). Dimethyl sulphoxide (DMSO) (99.7%) was obtained from Acros Organics (Geel, Belgium). HES ($\overline{M}_w = 130\,000\ g\ mol^{-1}$, degree of substitution (DS): 0.4) was a gracious gift of Fresenius Kabi Germany GmbH and Irgacure 2959 (I2959) was purchased from Ciba Specialty Chemicals Inc. (Basel, Switzerland). Polyethylene glycol with an average molecular weight of 12 000 g mol^{-1} (PEG 12 000) was purchased from Fluka (Steinheim, Germany) and monomeric mTagGFP was from Evrogen (Moscow, Russia). THF was dried over sodium and ethyl acetate was distilled before use. All other chemicals were used as received.

2.2. Synthesis of Polymers

Modified HES derivatives were synthesized as previously described[10] according to a general procedure by van Dijk Wolthuis et al.[33] In brief, HES-P(EG)$_n$MA ($n = 6$ or 10) was synthesized by a two-step synthesis where at first the imidazole carbamate (P(EG)$_n$MACI) was obtained after activation of P(EG)$_n$MA with CDI in THF. In the second step this group was coupled to the hydroxyethyl group of HES in DMSO using DMAP as catalyst, forming a carbonate ester linkage. The synthesis of the ester-linked HES-MA was performed in a one-step reaction via GMA and DMAP in DMSO also following a previously established method.[10] Different DS values were obtained by variation of HES and (P(EG)$_n$MACI) or GMA molar ratios or reaction time as can be seen in Table 1.

The DS of the HES backbone with the crosslinkable side chain was determined by ^{1}H-NMR spectroscopy according to Harling et al. by analyzing the proton ratio of the substituent's vinyl or methyl group to the CH_2-groups of the HES backbone.[7] The dried samples were dissolved in D_2O and spectra were recorded using a Bruker AM 400 NMR-spectrometer.

2.2.1. Synthesis of Lithium Phenyl-2,4,6-trimethylbenzoyl-phosphinate (LAP)

The initiator was synthesized according to Fairbanks et al.[34] Dimethyl phenylphosphonite (3.0 g, 0.018 mol) was added to a 250 mL flask under nitrogen. While stirring 2,4,6-trimethylphenylchloride (3.2 g, 0.018 mol) was added drop-wise. The reaction mixture was then stirred at room temperature (RT) and under nitrogen for 24 h. After heating the mixture to 50 °C, lithium bromide (6.2 g, 0.072 mol), dissolved in 100 mL of 2-butanone, was slowly added. After the mixture had been stirred at RT for 4 h the white-yellowish precipitate was washed with 2-butanone and dried.

2.2.2. Hydrogel Disks

The hydrogels were prepared using a pH 7.4 Sörensen phosphate buffer with initiator concentrations of 0.015, 0.05, and 0.1 wt% in the case of Irgacure 2959, or 0.01, 0.04, and 0.08 wt% of LAP. To obtain a gel disk of 2 cm diameter, the polymer was dissolved in 500 μL of an initiator solution to concentrations of 10, 20, and 30 wt%. For the fluorescence measurements 10 μL of mTagGFP solution (1 μg · μL^{-1}) were added and all were mixed for 15 min. The solutions were irradiated with UV light (366 nm, 3.0 mW · cm^{-2}) for 15 or 30 min.

2.2.3. Preparation of Hydrogel Microparticles

A general procedure described previously by Schwoerer et al. was used to prepare hydrogel microparticles via a water-in-water emulsion process.[6] One aqueous phase comprised 9.0 g of a 2 wt% HES-P(EG)$_6$MA solution, 0.9 g of a 0.1 wt% Irgacure 2959 solution and 10 μL of mTagGFP solution (1 μg · μL^{-1}), the second aqueous phase contained 6.0 g of PEG 12 000 solution (30 wt%) in 0.020 M sodium phosphate buffer pH 7.0. The two solutions were combined in a 20 mL glass vial. The glass vial was cooled to 0 °C for 10 min and subsequently mixed for one minute. The water-in-water emulsion obtained was exposed to UV light (366 nm) for 30 min. The resulting microparticles were washed three times with demineralized water and separated by centrifugation. The microparticles were characterized for their particle size distribution by laser diffraction (LS13320 PIDS, Beckman Coulter, Fullerton, CA). The encapsulation efficiency for GFP was calculated from the cumulative loss of the protein into the supernatants and the initially incorporated amount.

2.3. Analysis

2.3.1. Equilibrium Swelling

The influence of the initiator and polymer concentration on the crosslinking density was analyzed by swelling measurements. Freshly crosslinked, unloaded hydrogel disks were weighed and stored in pH 7.4 Sörensen phosphate buffer at 37 °C. The swelling gels were regularly re-weighed until the swelling equilibrium was reached. The swelling ratios (SWR) of the hydrogels were calculated

Table 1. Ratios and reaction times for DS adjustment of HES-P(EG)$_n$MA ($n = 6$ or 10) and HES-MA polymers.

HES-x	DS	Molar ratios					Reaction time [h]
		HES	P(EG)$_6$MACI	P(EG)$_{10}$MACI	GMA	DMAP	
MA	0.13	2	–	–	1	–	49
P(EG)$_6$MA	0.05	10	1	–	–	1	4
P(EG)$_6$MA	0.04	10	1	–	–	1	4
P(EG)$_6$MA	0.12	5	1	–	–	1	4
P(EG)$_{10}$MA	0.11	5	–	1	–	1	24

according to Peng et al.[35] by Equation 1.

$$SWR(\%) = \frac{W_s - W_d}{W_d} \cdot 100 \quad (1)$$

where W_s is the weight of the swollen hydrogel and W_d the weight of the hydrogel after freeze-drying.

2.3.2. Fluorescence Anisotropy

Observation of fluorescence anisotropy was done by excitation with linearly polarized light. Due to photoselection of excitation, emitting fluorophores show an alignment of emission dipoles resulting in fluorescence anisotropy.[36] The time-resolved fluorescence anisotropy $r(t)$ is defined as in Equation 2.

$$r(t) = \frac{I_{||}(t) - I_{\perp}(t)}{I_{||}(t) + 2I_{\perp}(t)} = \frac{D(t)}{F(t)} \quad (2)$$

Measuring two intensity decays I parallel and perpendicular to excitation polarization the time-resolved anisotropy $r(t)$ can be computed. The denominator includes the expression of the total fluorescence $F(t)$ from which the lifetime of the excited state of the fluorophore (short: fluorescence lifetime) can be extracted. Upon excitation with a δ-pulse (i.e., femtosecond pulses) an exponential decay of the anisotropy is observed, as described in Equation 3, where r_0 is the initial anisotropy that is constant for a certain fluorophore and excitation wavelength and θ_i stands for the rotational correlation time that describes the timescale on which anisotropic fluorescence is depolarized due to random rotational diffusion.

$$r(t) = r_0 \sum_i g_i \cdot e^{-\frac{t}{\theta_i}}, \ \sum_i g_i = 1 \quad (3)$$

The anisotropy decay may comprise several additive components with a fractional contribution g_i. They originate either from different detected fluorescent species, different moments of inertia for non-spherical molecules, or internal local motion of the fluorophore. The rotational correlation time θ is related to the size of the molecule M, the specific volume $\overline{V}$, the surrounding solvent viscosity η and volume V according to the Debye–Stokes–Einstein relationship Equation 4.

$$\theta = \frac{\eta V}{RT} = \frac{\eta M}{RT}\left(\overline{V} + h\right) \quad (4)$$

For biomolecules a tightly bound hydration shell h has to be taken into account that enlarges their apparent molecular size and may vary for different molecular environments. The rotational diffusion coefficient D_{rot} is related to the rotational diffusion time θ by the simple relationship given in Equation 5.

$$D_{rot} = (6\theta)^{-1} \quad (5)$$

Equation 5 holds only for spherical molecules. Although the shape of the GFP is more cylindrical only one component is detected since the moments of inertia are very similar and thus Equation 5 can be applied.

2.3.3. FRAP

FRAP measurements are based on the bleaching of fluorescent molecules inside a certain volume which generates a concentration gradient of the fluorophoric species. Subsequently, the recovery of the fluorescence in this area, driven by diffusion of unbleached molecules into and bleached molecules out of the bleaching volume, is monitored. FRAP allows for monitoring translational diffusion dynamics on a micrometer scale. In contrast to other fluorescence techniques investigating translational diffusion (i.e., fluorescence correlation spectroscopy and single particle tracking) both FRAP and anisotropy experiments can be conducted in the micromolar fluorophore regime, thus requiring only one sample. The fluorescence recovery can be described by solving Fick's second law of diffusion for simultaneous spatially and temporally changes of the concentration gradient C.

$$\frac{\partial}{\partial t} C(x,y,z,t) = D_{trans} \nabla^2 C(x,y,z,t) \quad (6)$$

This differential equation has to be solved with the appropriate initial and boundary conditions and related with the observed fluorescence profile. The main parameters are the bleaching kinetics, bleaching parameters as well as the bleaching geometry and the optical dimensions of the point spread function (PSF) of the microscope. When fitting the data to a model equation, the translational diffusion coefficient D_{trans} is obtained together with the bleaching depth or photobleaching parameter, respectively, and the mobile fraction of fluorescent molecules. Since the FRAP data in this work could not be successfully fitted to an adequate model equation,[24,37] a more simple approach was used for estimating D_{trans}. In this case, the width w of the sigmoid line profile of the transition from bleached to unbleached sample area as a function of time is computed. Differentiation of the intensity line profile yields a Gaussian-shaped curve as solution of Equation 6 for the one-dimensional case.

$$\begin{aligned} c(x,t) &= \frac{A}{\sqrt{4\pi \cdot D_{trans} t}} \cdot e^{-\frac{x^2}{4D_{trans}t}} \xleftarrow{w^2 = 2D_{trans}t} c(x,t) \\ &= \frac{A}{w(t)\sqrt{2\pi}} \cdot e^{-\frac{x^2}{2w(t)^2}} \end{aligned} \quad (7)$$

The profile width w is linked to D_{trans} by the Einstein–Smoluchowski relation (i.e., $w^2 = 2D_{trans}t$). The translational diffusion coefficient depends, as its rotational counterpart, on the molecular size and the solvent viscosity through the Stokes-Einstein relationship in Equation 8 where r_h designates the hydrodynamic radius of the molecule which explicitly includes the hydration shell of the protein.

$$D_{trans} = \frac{kT}{6\pi \cdot \eta \cdot r_h} \quad (8)$$

2.3.4. Anisotropy and FRAP Experimental Setup

Monomeric mTagGFP (238 amino acids, 27 kDa, from *Aequorea macrodactyla*, Evrogen, Moscow, Russia) was used.[38,39] Compared to wildtype GFP it possesses a S65C mutation in the chromophore. The one-photon absorption maximum is at $\lambda_{ex} = 483$ nm, the

maximum of emission at $\lambda_{em} = 506$ nm, the quantum yield is 0.6. The phenolic group of the chromophore has a pK_a of 5.0. Since the spectroscopic properties of mTagGFP are similar to EGFP (S65T mutation)[40] the two-photon absorption maximum was assumed to be within the same range. Blab et al. reported a two-photon action cross-section of 41 GM at 920 nm, Heikal et al. found 75 GM at 960 nm.[41,42] The instrumental setup used is shown in Figure 1.

A titanium-sapphire laser (Mira 900-D, 76 MHz, <200 fs; Coherent, Santa Clara, CA) was used at an excitation wavelength of 920 nm. The laser power was continuously attenuated by a half-wave plate and polarizing beamsplitter cube (P). The polarization was manipulated by a half-wave and quarter-wave plates (B. Halle Nachfl., Berlin, Germany) in order to obtain horizontally, vertically or circularly polarized light. After beam expansion a dichroic mirror (DC, T700 DCSPXR-UV; Chroma Technology, Bellows Falls, VT), reflects the excitation light which is focused by a 40× 1.30 nominal aperture (NA) oil immersion objective (EC Plan-Neofluar; Carl Zeiss Microimaging, Jena, Germany). The sample is scanned in the *x*-, *y*- and *z*-directions with two piezo scanners (P-733.2CL and P-721.CLQ (PIFOC); Physik Instrumente (PI), Karlsruhe, Germany). Fluorescence is colinearly collected by the objective, filtered by a Schott BG39 color filter and Semrock BrightLine FF01–530/40 interference filter (F_1 and F_2, IDEX, Lake Forest, IL), then split by a polarizing beamsplitter (P; Thorlabs, Dachau, Germany). Thus, parallel and perpendicularly emitted fluorescence light is simultaneously detected by two APD detectors (MPD, Bolzano, Italy). The signal is processed by a time-correlated single-photon counting unit (TCSPC, PicoHarp 300; PicoQuant, Berlin, Germany) with temporal synchronization via laser photodiode output.

For each anisotropy decay curve four intensity decay curves were recorded for correction of different detection efficiencies of the two detection pathways. The *G*-factor for co-linear excitation and detection, which corrects for these differences, was calculated according to Siegel et al.[43] The time-resolved intensity decays were transformed into fluorescence anisotropy and total intensity decay curves, respectively, according to Equation 2. With a non-linear fit routine (Levenberg–Marquardt iterative algorithm, OriginPro8; OriginLabs, Northampton, MA) a bi-exponential decay function according to Equation 3 with no offset was fitted to the data which yielded rotational correlation times θ and fluorescence lifetimes τ.

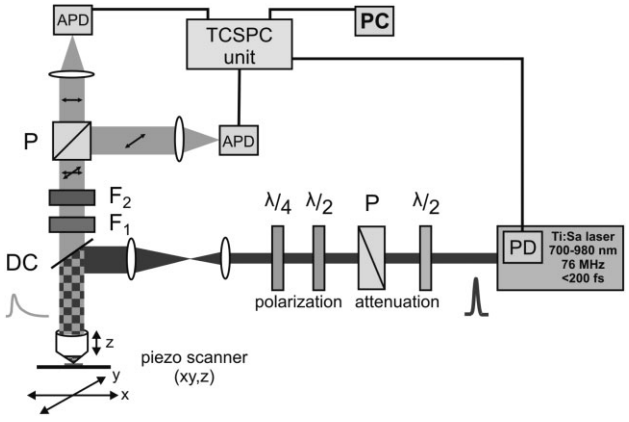

Figure 1. Experimental setup for 2-photon anisotropy and FRAP measurements. For abbreviations see text.

The latter were mainly used to verify the source of fluorescence originating from intact mTagGFP protein. Errors are given as standard deviation, error propagation was calculated applying Gaussian error distribution.

Although no polarization information is needed for FRAP experiments, the same setup was used. Thus, both examination methods could be applied on one sample without changing the setup. For FRAP bleaching the excitation power was turned up to 50 mW (measured under objective) and the detection pathway was blocked in order to avoid damaging of sensitive APD detectors. An area of approximately 5 μm × 5 μm was bleached. After bleaching the excitation power was turned down to recovery measurement level (4–5 mW) and the detection pathway was unblocked. Due to very long recording times (up to 3 h) sample drifting occurred. Lateral drifting could be compensated in image analysis by manually shifting the region of interest whereas image series with axial drifting (focus drift) had to be discarded. Since this process often occurred discontinuously it could be distinguished from the continuous diffusion process.

3. Results and Discussion

3.1. Hydrogel Characteristics

The basic polymer was HES which has been in use as plasma expander for over 40 years.[44] This degradable polymer was modified with P(EG)$_n$MA or MA to incorporate a crosslinkable double bond and to enhance water solubility. Degradation of the sidegroup is also possible due to the carbonate ester linkage in the case of HES-P(EG)$_n$MA whereas HES-MA has a more stable ester linkage.[33,45] The protein loaded hydrogels were prepared by photo crosslinking of polymer solution containing mTagGFP and low amounts of the photoinitiators Irgacure 2959 or LAP (Figure 2). Both initiators can be applied with irradiation of 366 nm and have demonstrated good cytocompatibility as previously investigated by Fairbanks et al. with human neonatal foreskin fibroblast cells.[34] Identical cell viabilities (ca. 95%) were obtained after 24 h.

3.2. Characterization of Unloaded Hydrogels

Since a low drug mobility and prolonged release were desired, all important parameters for the crosslinking process were optimized to achieve a high network density. The influence of initiator and polymer concentration as well as the UV-irradiation time on the network density of the hydrogels was analyzed by swelling measurements. Because the photoinitiators form radicals that might damage the incorporated proteins, their concentration has to be kept low.[46] Hence both photoinitiators used for hydrogel preparation were tested regarding the influence of concentration on the swelling ratio of HES-P(EG)$_6$MA gels (Figure 3).

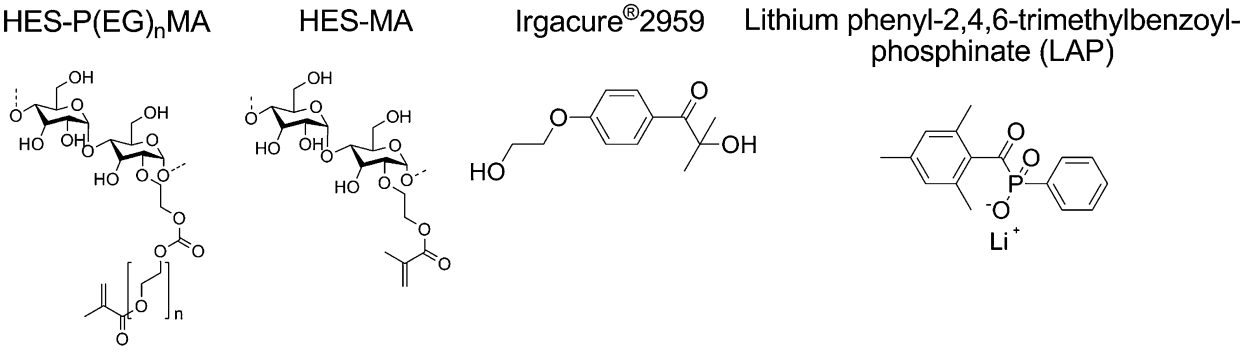

Figure 2. HES derivatives and the photoinitiators used for the preparation of hydrogels and hydrogel microparticles (Irgacure 2959 only).

Using LAP at different concentrations (Figure 3A) led to a slightly lower water uptake at higher concentrations. Hydrogels prepared with different Irgacure 2959 (I2959) concentrations exhibited comparable swelling ratios (Figure 3B). Thus for both initiators the lowest concentration was already sufficient to obtain hydrogels with a high crosslinking density after the given irradiation time. Although lower initiator concentrations were used, hydrogels prepared with LAP showed a lower swelling ratio than gels with Irgacure 2959. This is caused by the higher initiation rate of LAP at 366 nm. The initiation rate (Equation 9)

$$R_i = \frac{2\phi\varepsilon f l C_i}{N_A h \nu} \tag{9}$$

is proportional to the quantum yield ϕ, initiator efficiency f, light intensity l, the initiator concentration C_i and the molar extinction coefficient ε. Here N_A is the Avogadro number, h the Planck constant and ν the light frequency.[47] Fairbanks et al. demonstrated that quantum yield, initiator efficiency and the light absorption of LAP are superior to I2959 at 366 nm, leading to a higher performance.[34] This effect is even enhanced in thicker samples due to the lower light absorption of the cleavage products of LAP. In this case more light is able to penetrate deeper into the sample. However, I2959 forms radicals with nearly the same absorption, which lowers the possibility of photocleavage deeper in the hydrogel.[34] Consequently, a shorter irradiation time could be applied using LAP instead of Irgacure 2959 during crosslinking to obtain the same network density. Due to this fact and its better water solubility and comparable cytocompatibility,[34] 0.01 wt% LAP were mainly used to prepare hydrogels for the fluorescence measurements. Secondly, the influence of irradiation time on the water uptake was studied. Longer irradiation times could even lead to a lower network density, like it was observed for an irradiation time of 30 min (Figure 4).

Comparing irradiation times of 15 and 30 min showed lower swelling ratios after 15 min for 10 wt% and

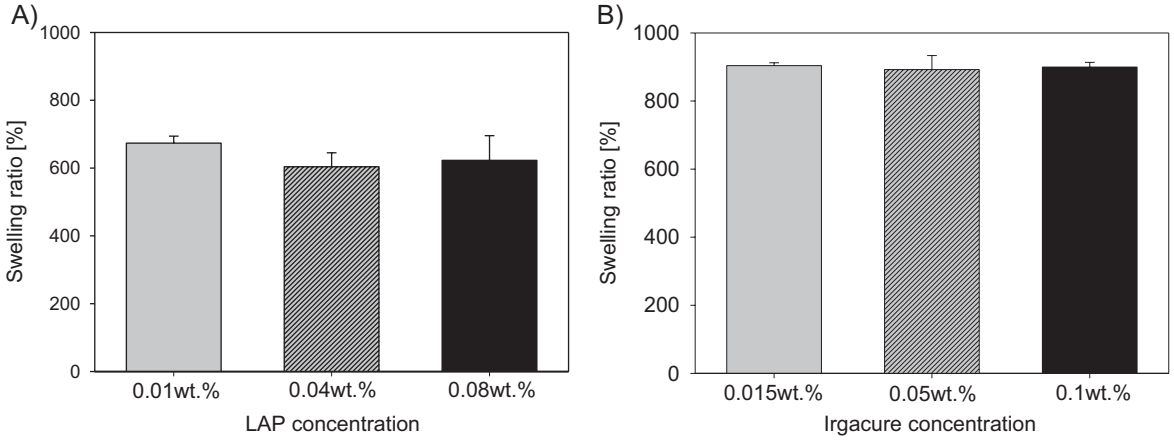

Figure 3. Swelling ratios of 20 wt% HES-P(EG)$_6$MA hydrogels produced by 15 min irradiation at 366 nm with different LAP (A) and Irgacure 2959 (B) initiator concentrations at swelling equilibrium (measurement after 165 h in (A) and after 65 h in (B)). Data are shown as means ± standard deviations ($n = 3$).

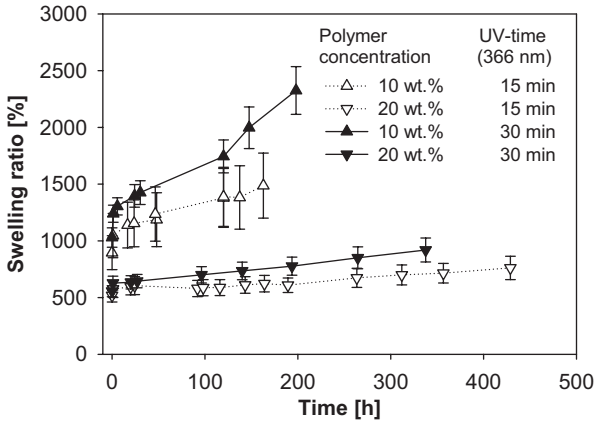

Figure 4. Swelling ratios of HES-P(EG)$_6$MA gels prepared with 0.08 wt% LAP, varying polymer concentrations and UV-irradiation times as function of time. 10 wt% gels decomposed into several pieces after ca. 200 h. Data are shown as means ± standard deviations ($n = 3$).

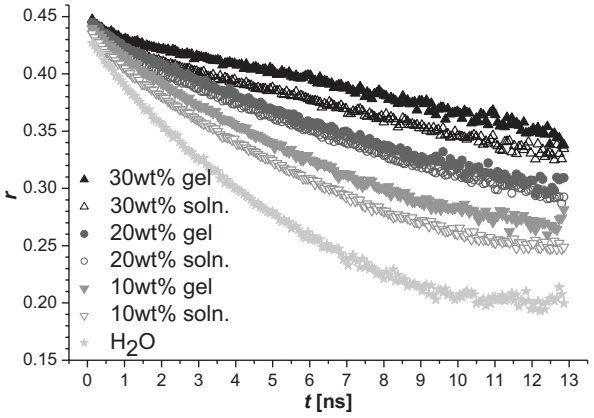

Figure 5. Anisotropy (r) decay curves as function of time (t) (2-photon excitation) for mTagGFP in HES-P(EG)$_6$MA (DS = 0.05) hydrogels (gel) with different polymer concentrations and for the corresponding prepolymer solutions (soln.) as well as in water. All curves are based on mean values derived from five individual measurements. Error bars are omitted for clarity and are in the range of 0.1–2%.

20 wt% HES-P(EG)$_6$MA hydrogels, respectively. Instead of an increase in crosslinking density, due to newly formed radicals, the opposite effect was observed. Radicals formed after 15 min possibly damaged the polymer network or caused cyclization or termination reactions.[48] Similar results have been reported for PEG diacrylate hydrogels by Mironi–Harpaz et al.[49] However, the UV-irradiation time was chosen as 30 min instead of 15 min due to increased light scattering and possible light absorption caused by the GFP. Figure 4 also shows that an increase in polymer concentration from 10 wt% to 20 wt% considerably lowered the swelling ratio. Since a low swelling ratio points to a high network density the hydrogels consisting of 20 wt% should be strongly crosslinked.

3.3. Fluorescence Anisotropy Experiments

The influence of several hydrogel parameters on the rotational mobility of mTagGFP in the hydrogel network was investigated. The corresponding rotational correlation times θ were extracted from the decay curves by a fitting procedure as described before. Two rotational components were found. The mTagGFP protein exhibited a partial segmental motion of the chromophore θ_1 (cf. Figure 5). The rotational correlation time for this local rotation ranged around 1 ns with approximately 4% contribution to the anisotropy decay. It is insensitive to the molecular environment of the protein since the chromophore is buried within the β-barrel. A similar observation has been made by Liu et al. with GFP-S65T.[50] Therefore in all further discussions only the long rotational correlation time θ_2 is mentioned which can be ascribed to the globular protein rotation and which is sensitive to the molecular environment. Quantitative data from curve fitting for all measurements is summarized in Table 2 which is discussed in the following paragraphs. The rotational diffusion coefficient D_{rot} and the viscosity η_{rot} are derived from Equation 5 and Equation 4, respectively by employing sucrose reference samples with known viscosity (see text below).[51]

The first investigated parameter, with respect to rotational mobility, was the polymer concentration since the swelling measurements had revealed an increase in network density with increasing polymer concentration (Figure 4). The anisotropy decay curves in Figure 5 indicate an increased rotation retardation of mTagGFP when the polymer concentration was increased from 10 to 30 wt% polymer. All hydrogel curves lie considerably above the decay curve for pure water (Table 2, row 1). In order to determine the origin of this effect hydrogels were compared with non-crosslinked polymer solutions (Table 2, row 2, 9, 11; Figure 5).

A small increase in rotational retardation could be observed due to crosslinking which was statistically significant for 10 and 30 wt% hydrogels, respectively. However, the difference in the decay curves for crosslinked and non-crosslinked solutions of the same concentration was small compared to the influence of the polymer concentration. It can be concluded that the main influence of rotation retardation is due to viscosity caused by the increase of the polymer concentration, (i.e., an increase in the number of molecular interactions between the GFP and the polymer chains). Crosslinking had only a minor effect. Adsorption or binding of the protein to the polymer matrix cannot be completely excluded. However, due to the findings it is expected to play a negligible role as a much larger influence on the retardation of rotation would be

Table 2. Selected curve fit results (θ_2, reduced χ^2, adjusted R^2) for mTagGFP anisotropy decay in all investigated HES-P(EG)$_n$MA hydrogels (gel), microparticles (part.), solutions (soln.) and water. The polymer solutions did not contain any initiators and were not UV irradiated. All experiments were conducted at 20 °C.

	Sample type	Polymer [wt%]	n	DS	Initiator	θ_2 [ns]	χ^2_{red}	$\overline{R}^2$	D_{rot} [$\times 10^6 s^{-1}$]	η_{rot} [mPa·s]
1	H_2O	–	–	–	–	14.0 ± 0.5	0.99	0.9993	11.9 ± 0.5	1.00
2	soln.	10	6	0.05	–	19.8 ± 0.2	1.47	0.9995	8.4 ± 0.1	1.55 ± 0.04
3	gel	10	6	0.05	LAP	22.9 ± 0.5	1.09	0.9990	7.3 ± 0.2	1.85 ± 0.07
4	gel	10	6	0.12	LAP	22.8 ± 0.3	1.46	0.9993	7.3 ± 0.1	1.83 ± 0.06
5	gel	10	0	0.13	LAP	22.6 ± 0.2	1.12	0.9993	7.4 ± 0.1	1.82 ± 0.05
6	gel	10	10	0.11	LAP	22.9 ± 0.3	1.36	0.9992	7.3 ± 0.1	1.85 ± 0.06
7	gel	20	6	0.05	I2959	33.2 ± 0.4	1.06	0.9980	5.0 ± 0.1	2.87 ± 0.09
8	gel	20	6	0.05	LAP	31.0 ± 0.4	1.40	0.9977	5.4 ± 0.1	2.65 ± 0.08
9	soln.	20	6	0.05	–	31.1 ± 0.3	1.43	0.9991	5.4 ± 0.1	2.65 ± 0.08
10	gel	30	6	0.05	LAP	62.5 ± 1.0	1.10	0.9940	2.7 ± 0.1	>4[a]
11	soln.	30	6	0.05	–	48.9 ± 0.7	1.32	0.9971	3.4 ± 0.1	>4[a]
12	part.	≈25[b]	6	0.04	I2959	38.2 ± 3.7	1.18	0.9775	4.4 ± 0.4	3.38 ± 0.39

[a] The actual viscosities for a 30 wt% hydrogel and polymer solution are out of the linear θ–η range (see text); [b] This is the concentration determined by comparison of anisotropy decay in hydrogel microparticles and disks (see text), though for preparation of particles a 2 wt% solution was used.

expected in the case of protein binding to the polymer matrix.

In order to obtain more information about the influence of the viscosity on the rotational diffusion of GFP sucrose solutions were used as reference with known viscosity. Sucrose is chemically very similar to the HES backbone and, as a consequence, similar molecular interactions may be assumed. It should be mentioned that sucrose will not cause denaturation of GFP even at high concentrations.[52,53] Figure 6 shows a plot of the global rotational correlation time θ_2 as a function of viscosity as determined from the measurements with sucrose solutions.

A near-linear relationship (slope 0.84 in a double logarithmic plot) was found up to approximately 4 mPa · s s between rotational correlation time θ and viscosity η according to Equation 4. Applying a linear regression permitted the determination of the local microscopic viscosity η_{rot} within the hydrogels. The absolute θ-values were in good agreement with results from Suhling et al. for EGFP in sucrose and fructose solutions.[19] For higher viscosities a strong deviation from the linear Debye-Stokes-Einstein relationship was observed. Similar observations were made by Chuang and Eisenthal for the organic dye rhodamine 6G in aliphatic alcohols.[54] Solvents with considerable hydrogen bonding contribution to shear viscosity may strongly deviate from the simple linear relationship. In addition, the hydration shell of the protein may vary for highly concentrated sucrose solutions which would probably result in a reduced total size of the protein-hydration shell complex. Furthermore, the determination of θ for slow fluorescence depolarization is afflicted with high uncertainties due to the comparatively short lifetime of the excited state of the fluorophore.

The next investigated parameter was the influence of the ethylene glycol (EG) spacer length of the prepolymer between HES backbone and MA group. It was examined

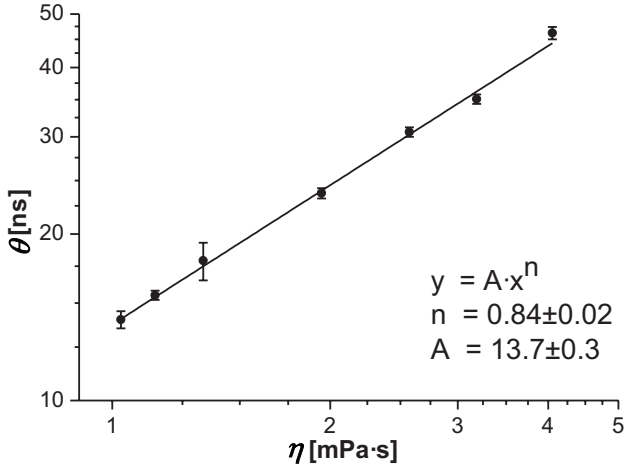

Figure 6. Calibration function showing the relationship between rotational correlation time θ_2 and viscosity η determined with sucrose solutions.[50]

by comparing the hydrogels with six, ten and no EG units (cf. Table 2, row 4–6). Their DS was slightly different but was assumed to have a minor influence on the results. All three hydrogels showed almost identical anisotropy decay behavior and thus no influence of spacer length on the rotational mobility of incorporated GFP molecules. Comparable results were found for the influence of the DS value. The anisotropy decay of GFP in two hydrogels with a DS of 0.048 and 0.12, respectively, was indistinguishable (cf. Table 2, row 3 and 4). This confirms the hypothesis that rotational diffusion retardation was mainly governed by interaction with the starch backbone, not by crosslinking.

Another parameter under investigation was the use of different initiators. Two 20 wt% HES-P(EG)$_6$MA (DS = 0.05) prepolymer solutions were crosslinked with either I2959 or LAP. The anisotropy decay of both hydrogels lay within the statistical uncertainties and hence could not be distinguished (cf. Table 2, row 7 and 8).

Fluorescence anisotropy decay was also studied for hydrogel microparticles since their way of preparation is completely different from that of hydrogel disks. While disks were made from bulk solutions, microparticles were prepared in a water-in-water emulsion process. The encapsulation efficiency of the mTagGFP in microparticles was determined to be 83%. Laser diffraction measurements yielded a unimodal particle size distribution with a median of 9.7 μm. The uniform protein distribution within the particles was qualitatively verified by two-photon excitation fluorescence microscopy and was in good agreement to earlier investigations on fluorescein isothiocyanate (FITC)-dextran loaded microparticles.[6] In Figure 7 the anisotropy decay curve for microparticles is qualitatively compared to the decay curves resulting from hydrogel disk experiments.

A very important result is that although the microparticles were produced with a 2 wt% prepolymer solution, their anisotropy decay curve lay in between the curves for hydrogel disks prepared with 20 and 30 wt% polymer which is quantitatively confirmed (cf. Table 2, row 12). Hence, it could be concluded that water migrates from the HES-P(EG)$_6$MA to the PEG phase during the microparticle preparation process and the polymer is concentrated within the evolving microparticles. The polymer concentration of the HES-P(EG)$_6$MA microparticles at the time point of crosslinking, which cannot be measured directly in this case, is approximately 25%.

3.4. FRAP Experiments

By conducting FRAP experiments on mTagGFP loaded hydrogels it was possible to determine the D_{trans} and thus the translational mobility of the model protein GFP within the hydrogel network. A representative image series for a 30 wt% hydrogel is displayed in Figure 8.

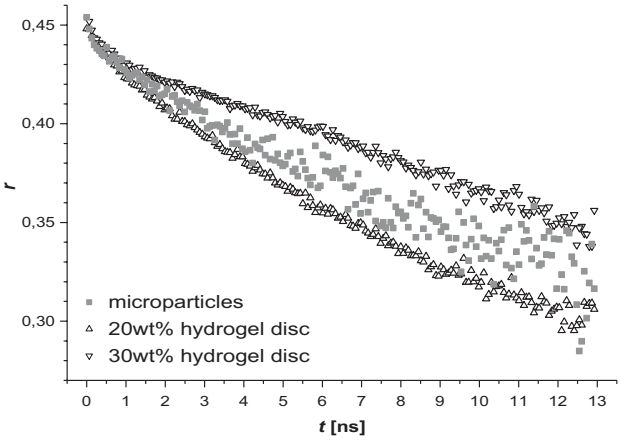

Figure 7. Anisotropy (r) decay curve as function of time (t) (2-photon excitation) for HES-P(EG)$_6$MA (DS = 0.04) microparticles prepared with 0.1 wt% I2959 and 2 wt% HES-P(EG)$_6$MA solution in comparison to that of HES-P(EG)$_6$MA (DS = 0.05) hydrogel disks of different polymer concentration prepared with 0.01 wt% LAP. The microparticles curve was arbitrarily y-shifted by 0.02 units for a better comparison of the anisotropy decays. Error bars are omitted for clarity.

Even after almost three hours of fluorescence recovery the bleached area was distinctively visible. Besides a slight brightening of the bleached area two other processes became noticeable. Firstly, the generation of a small boss at the right bottom of the bleached square was observed. This might be ascribed to a microchannel or a gel inhomogeneity that allows faster diffusion of the species in this direction. Secondly, the edge of the bleached area became blurrier due to diffusion. The application of a mathematical recovery model for the time dependent fluorescence intensity distribution, for example, from Mazza et al.[24] for 3D diffusion and multiphoton excitation could not be fitted to the data due to time limitations. Although the fluorescence pattern was recorded for almost three hours,

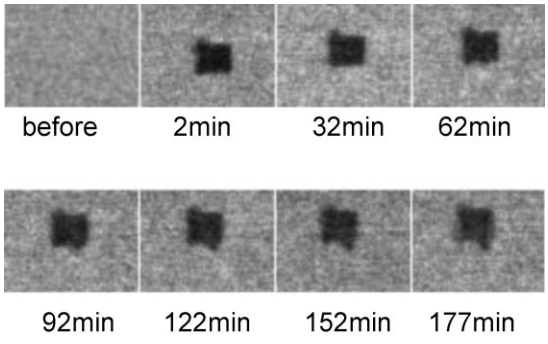

Figure 8. Image time lapse of a 3 h FRAP experiment with mTagGFP in 30 wt% HES-P(EG)$_6$MA hydrogel. The upper left image shows the imaged area before bleaching, the other images were recorded after the denoted elapsed time after photobleaching.

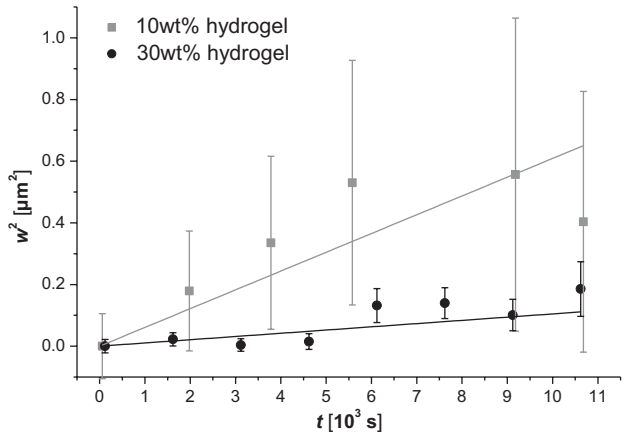

Figure 9. Weighted linear regression for the squared intensity profile width w^2 over time (cf. Equation 7) for the determination of the translational diffusion coefficient of a 10 wt% and 30 wt% HES-P(EG)$_6$MA/DS0.048/0.01 wt% LAP hydrogel. The profile widths are arbitrarily set to zero for $t = 0$.

this time frame only comprised the very beginning of the recovery process which entails a high uncertainty when fitting the model equation to the data points. In most experiments, the FRAP process is completed within milliseconds up to a few minutes and can therefore be repeated several times in order to obtain a high signal-to-noise ratio. This approach is not practicable for extremely slow fluorescence recoveries. In order to achieve an estimation of D_{trans} in reasonable time, the broadening of the intensity profile across the border of bleached and unbleached area was fitted to Equation 7. By using the Einstein–Smoluchowski relation D_{trans} can be derived by fitting the evolution of the squared intensity profile width w^2 over time. The resulting data points of this method for a 10 wt% and 30 wt% HES-P(EG)$_6$MA hydrogel are displayed in Figure 9 together with a weighted linear regression.

Although the error is large for single data points, the trend clearly shows that translational diffusion was decreased with increasing polymer concentration of the hydrogel. The uncertainties for the 10 wt% hydrogel measurement are considerably higher, probably due to a less distinct border between bleached and unbleached area in the recorded images. The computed D_{trans} values are shown in Table 3 and compared with diffusion coefficients of GFP in water as well as in other hydrogel systems. The viscosities were calculated according to Equation 8 using the hydrodynamic radius determined from fluorescence anisotropy measurements and assuming it to be the same for translation and rotation.

The time series in Figure 8 together with the quantitative values of D_{trans} in Table 3 unambiguously illustrate that mTagGFP was effectively retained in the hydrogel. The translational diffusion was about six orders of magnitude lower than for wildtype GFP in water.[25] Compared with the diffusion of larger molecules in other types of hydrogels (i.e., 144 kDa IgG[55] and 2 MDa dextran),[23] diffusion of GFP still occurred several orders slower. Diffusion on a similar scale has recently been shown by Wells et al. with slightly smaller lysozyme (14.4 kDa) in a photo-responsive PEG-anthracene grafted hyaluronan hydrogel.[56] Although the accuracy of the experimental data needs to be improved, effective immobilization of GFP was unambiguously demonstrated.

Comparing the computed viscosities from anisotropy and FRAP data (Equation 4 and Equation 8, respectively) there is a huge discrepancy for the two values. However, it has to be mentioned that viscosity is a macroscopically defined quantity. On a microscopic scale the molecular friction is different for intrapore rotation and interpore translation. While the rotational diffusion of the molecule was only moderately restricted by friction, the 3D polymer network greatly affected the translational mobility on a micrometer scale. A similar finding has been reported by Hungerford et al. in a silica sol–gel matrix.[20] In order to prove that the immobilization of the enclosed protein is caused by the formation of a polymer network, non-crosslinked polymer solutions were investigated in an additional FRAP experiment as shown in Figure 10.

Table 3. Translational diffusion coefficients and calculated viscosities for mTagGFP in the hydrogels under investigation derived from FRAP and comparison with data from literature.

	D_{trans} [µm$^2 \cdot$ s^{-1}]	η_{trans} [mPa $\cdot$ s]	Reference
27 kDa mTagGFP in 30 wt% HES-P(EG)$_6$MA	$(0.5 \pm 0.2) \times 10^{-5}$	$\approx 18 \cdot 10^6$	this work
27 kDa mTagGFP in 10 wt% HES-P(EG)$_6$MA	$(3.0 \pm 1.3) \times 10^{-5}$	$\approx 3 \cdot 10^6$	this work
27 kDa wtGFP in H_2O	$(8.7 \pm 1.7) \times 10^{1}$		Brown et al.[25]
2000 kDa FITC-dextran in 10% PEG-hydrogel	$(1 \pm 0) \times 10^{-1}$		Brandl et al.[23]
144 kDa IgG-FITC in 4% galactoside-hydrogel	$(3.3 \pm 1.5) \times 10^{1}$		Markowitz et al.[55]
14.4 kDa lysozyme in hyaluronan photogel	1.8×10^{-3} a) 4.6×10^{-5} b)		Wells et al.[56]

a)Value taken right after laser irradiation which triggers release; b)Value taken 146 min post laser treatment.

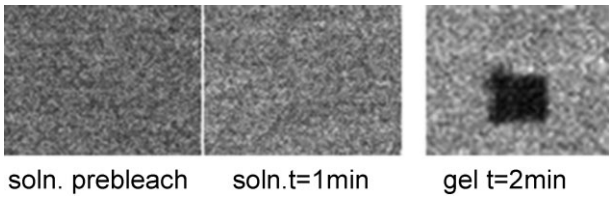

Figure 10. FRAP experiment for 30 wt% HES-P(EG)$_6$MA polymer solution with mTagGFP, left: prebleach image, middle: postbleach image, right: postbleach image for the corresponding crosslinked hydrogel for comparison.

Due to hardware restrictions (piezo-scanner, manual power adjustment) the first images after bleaching could only be recorded about one minute after the end of bleaching process. After this time period, fluorescence intensity had completely recovered within the bleached area for HES-P(EG)$_6$MA polymer solutions. Therefore, diffusion in non-crosslinked polymer solutions was very fast compared to hydrogels. The full recovery of fluorescence additionally indicated that the mobile fraction was close to unity. This finding confirmed that formation of a polymer network effectively immobilized translational diffusion of the entrapped protein on a micrometer scale.

In order to observe the fast fluorescence recovery for a polymer solution, the intensity-time profile was recorded with a stationary beam at a bleaching power of 50 mW and 10% fluorescence attenuation. By on-off switching cycles of the laser the recovery time can be estimated. The data for a 30 wt% HES-P(EG)$_6$MA prepolymer solution (not shown) revealed that the initial intensity was completely recovered within a few seconds. Similar behavior was observed for mTagGFP in 50 wt% sucrose solution. On the other hand, no fluorescence bleaching and thus fluorescence recovery could be observed for a 20 wt% polymer solution and for mTagGFP in water with 1 ms time resolution as translational diffusion was so fast that bleached GFP was completely replaced by new GFP molecules within a millisecond (cf. work of Brown et al.[25]).

4. Conclusion

The influence of crosslinking parameters on the network density of hydrogels prepared from modified HES, HES-P(EG)$_6$MA, by photo crosslinking with Irgacure 2959 or LAP was tested by swelling measurements. The gel properties could easily be tailored by variation of polymer concentration. Because initiator concentration and UV irradiation time showed only minor influences on network density, both can be kept low to minimize the damage of the incorporated protein.

The mobility of incorporated mTagGFP in the hydrogels prepared under optimized conditions was analyzed by fluorescence studies. Fluorescence anisotropy experiments showed that the incorporated protein was rotating relatively unhindered. The main retardation in rotational diffusion could be attributed to an increase in viscosity of the surrounding medium with increasing polymer concentration of the hydrogels. Comparing crosslinked polymers and non-crosslinked polymer solution revealed that crosslinking adds only a minor contribution on the rotational retardation of GFP. Accordingly, spacer length and DS did not influence the rotational mobility within the investigated range. Therefore the data indicate that any substantial adsorption or binding of the protein to the polymer network is not probable or at least a large fraction of the protein molecules is freely rotating.

FRAP measurements on the other hand demonstrated very effective immobilization of GFP molecules on a micrometer scale. An influence of the polymer concentration in the hydrogel on the degree of immobilization was observed. A good estimation of D_{trans} could be made with a simplified diffusion model. The hydrogel systems based on modified HES indicated a very slow diffusion compared to other hydrogel systems. This is in accordance with in vitro release studies in phosphate buffer at pH 7.4, which showed a release of FITC-dextrans of various sizes over months.[57] Anisotropy and FRAP measurements in combination with traditional methods of gel characterization could provide valuable complementary information about protein mobility in a short time and might help to obtain an estimate of the release behavior.

Acknowledgements: This research was financially supported by the DFG as part of the SFB 578. Support from the IGSM Braunschweig is gratefully acknowledged.

Received: September 3, 2012; Revised: October 30, 2012; Published online: December 17, 2012; DOI: 10.1002/mabi.201200325

Keywords: drug delivery systems; FRAP; GFP; hydrogels; two-photon fluorescence anisotropy

[1] A. S. Hoffman, *Adv. Drug Delivery Rev.* **2002**, *54*, 3.
[2] T. R. Hoare, D. S. Kohane, *Polymer* **2008**, *49*, 1993.
[3] P. Goddard, *Adv. Drug Delivery Rev.* **1991**, *6*, 103.
[4] J. W. Larrick, *Pharmacol. Rev.* **1989**, *41*, 539.
[5] C.-C. Lin, K. S. Anseth, *Pharm. Res.* **2009**, *26*, 631.
[6] A. D. A. Schwoerer, S. Harling, K. Scheibe, H. Menzel, R. Daniels, *Eur. J. Pharm. Biopharm.* **2009**, *73*, 351.
[7] S. Harling, A. Schwoerer, K. Scheibe, R. Daniels, H. Menzel, *J. Microencapsul.* **2010**, *27*, 400.
[8] J. Siepmann, J. Göpferich, *Adv. Drug Delivery Rev.* **2001**, *48*, 229.
[9] M. C. Bonferoni, S. Rossi, F. Ferrari, E. Stavik, A. Pena-Romero, C. Caramella, *AAPS PharmSciTech.* **2000**, *01*, e15.
[10] S. Wöhl-Bruhn, A. Bertz, S. Harling, H. Menzel, H. Bunjes, *Eur. J. Pharm. Biopharm.* **2012**, *81*, 573.

[11] J. R. Lakowicz, H. Szmacinski, K. Nowaczyk, M. L. Johnson, *Proc. Natl. Acad. Sci. USA* **1992**, *89*, 1271.
[12] W. R. Zipfel, R. M. Williams, R. Christie, A. Y. Nikitin, B. T. Hyman, W. W. Webb, *Proc. Natl. Acad. Sci. USA* **2003**, *100*, 7075.
[13] M. Rubart, *Circ. Res.* **2004**, *95*, 1154.
[14] R. Niesner, B. Peker, P. Schlüsche, K.-H. Gericke, C. Hoffmann, D. Hahne, C. Müller-Goymann, *Pharm. Res.* **2005**, *22*, 1079.
[15] R. Carriles, D. N. Schafer, K. E. Sheetz, J. J. Field, R. Cisek, V. Barzda, A. W. Sylvester, J. A. Squier, *Rev. Sci. Instrum.* **2009**, *80*, 81.
[16] W. R. Zipfel, R. M. Williams, W. W. Webb, *Nat. Biotechnol.* **2003**, *21*, 1369.
[17] P. T. C. So, C. Y. Dong, B. R. Masters, K. M. Berland, *Annu. Rev. Biomed. Eng.* **2000**, *2*, 399.
[18] K. Suhling, P. M. W. French, D. Phillips, *Photochem. Photobiol. Sci.* **2005**, *4*, 13.
[19] K. Suhling, D. M. Davis, D. Phillips, *J. Fluoresc.* **2002**, *12*, 91.
[20] G. Hungerford, A. Rei, M. I. C. Ferreira, K. Suhling, C. Tregidgo, *J. Phys. Chem. B* **2007**, *111*, 3558.
[21] D. Axelrod, D. E. Koppel, J. Schlessinger, E. Elson, W. W. Webb, *Biophys. J.* **1976**, *16*, 1055.
[22] M. C. Branco, D. J. Pochan, N. J. Wagner, J. P. Schneider, *Biomaterials* **2009**, *30*, 1339.
[23] F. Brandl, F. Kastner, R. M. Gschwind, T. Blunk, J. Teßmar, A. Göpferich, *J. Controlled Release* **2010**, *142*, 221.
[24] D. Mazza, K. Braeckmans, F. Cella, I. Testa, D. Vercauteren, J. Demeester, S. S. Smedt, A. Diaspro, *Biophys. J.* **2008**, *95*, 3457.
[25] E. B. Brown, E. S. Wu, W. Zipfel, W. W. Webb, *Biophys. J.* **1999**, *77*, 2837.
[26] S. Andrade, S. Costa, J. Borst, A. Hoek, A. Visser, *J. Fluoresc.* **2008**, *18*, 601.
[27] S. A. Weinreis, J. P. Ellis, S. Cavagnero, *Methods* **2010**, *52*, 57.
[28] M. Ormö, A. B. Cubitt, K. Kallio, L. A. Gross, R. Y. Tsien, S. J. Remington, *Science* **1996**, *273*, 1392.
[29] M. Zimmer, *Chem. Rev.* **2002**, *102*, 759.
[30] W. E. Hennink, C. F. van Nostrum, *Adv. Drug Delivery Rev.* **2002**, *54*, 13.
[31] N. A. Peppas, *Curr. Opin. Colloid Interfaces* **1997**, *2*, 531.
[32] R. J. H. Stenekes, W. E. Hennink, *Int. J. Pharm.* **1999**, *189*, 131.
[33] W. N. E. van Dijk-Wolthuis, J. A. M. Hoogeboom, M. J. van Steenbergen, S. K. Y. Tsang, W. E. Hennink, *Macromolecules* **1997**, *30*, 4639.
[34] B. D. Fairbanks, M. P. Schwartz, C. N. Bowman, K. S. Anseth, *Biomaterials* **2009**, *30*, 6702.
[35] T. Peng, K. de Yao, C. Yuan, M. F. A. Goosen, *J. Polym. Sci., Polym. Chem.* **1994**, *32*, 591.
[36] J. R. Lakowicz, *Principles of Fluorescence Spectroscopy*, Springer, New York, NY **2006**.
[37] E. A. Schnell, L. Eikenes, I. Tufto, A. Erikson, A. Juthajan, M. Lindgren, C. de Lange Davies, *J. Biomed. Opt.* **2008**, *13*, 64037.
[38] N.-S. Xia, W.-X. Luo, J. Zhang, X.-Y. Xie, H.-J. Yang, S.-W. Li, M. Chen, M.-H. Ng, *Mar. Biotechnol.* **2002**, *4*, 155.
[39] O. M. Subach, I. S. Gundorov, M. Yoshimura, F. V. Subach, J. Zhang, D. Grüenwald, E. A. Souslova, D. M. Chudakov, V. V. Verkhusha, *Chem. Biol.* **2008**, *15*, 1116.
[40] G. Patterson, R. N. Day, D. Piston, *J. Cell. Sci.* **2001**, *114*, 837.
[41] G. A. Blab, P. H. M. Lommerse, L. Cognet, G. S. Harms, T. Schmidt, *Chem. Phys. Lett.* **2001**, *350*, 71.
[42] A. A. Heikal, S. T. Hess, W. W. Webb, *Chem. Phys.* **2001**, *274*, 37.
[43] J. Siegel, K. Suhling, S. Lévêque-Fort, S. E. D. Webb, D. M. Davis, D. Phillips, Y. Sabharwal, P. M. W. French, *Rev. Sci. Instrum.* **2003**, *74*, 182.
[44] P. Lawin, J. Zander, B. Weidler, *Hydroxyethyl Starch: A Current Overview*, G Thieme, Stuttgart **1992**.
[45] W. N. E. van Dijk-Wolthuis, M. J. van Steenbergen, W. J. M. Underberg, W. E. Hennink, *J. Pharm. Sci.* **1997**, *86*, 413.
[46] C.-C. Lin, S. M. Sawicki, A. T. Metters, *Biomacromolecules* **2007**, *9*, 75.
[47] J.-P. Fouassier, *Photoinitiation, Photopolymerization and Photocuring: Fundamentals and Applications*, Carl Hanser, Munich **1995**.
[48] H. J. Naghash, O. Okay, Y. Yağci, *Polymer* **1997**, *38*, 1187.
[49] I. Mironi-Harpaz, D. Y. Wang, S. Venkatraman, D. Seliktar, *Acta Biomater.* **2012**, *8*, 1838.
[50] Y. Liu, H.-R. Kim, A. A. Heikal, *J. Phys. Chem. B* **2006**, *110*, 24138.
[51] D. R. Lide, CRC Handbook of Chemistry and Physics, A Ready-Reference Book of Chemical and Physical Data, CRC Press, Boca Raton, FL **2001**.
[52] F. Yang, L. G. Moss, G. N. Phillips, *Nat. Biotechnol.* **1996**, *14*, 1246.
[53] A. B. Cubitt, R. Heim, S. R. Adams, A. E. Boyd, L. A. Gross, R. Y. Tsien, *Trends Biochem. Sci.* **1995**, *20*, 448.
[54] T. J. Chuang, K. B. Eisenthal, *Chem. Phys. Lett.* **1971**, *11*, 368.
[55] M. A. Markowitz, D. C. Turner, B. D. Martin, B. P. Gaber, *Appl. Biochem. Biotech.* **1997**, *68*, 57.
[56] L. A. Wells, S. Furukawa, H. Sheardown, *Biomacromolecules* **2011**, *12*, 923.
[57] A. Bertz, S. Wöhl-Bruhn, S. Miethe, B. Tiersch, J. Koetz, M. Hust, H. Bunjes, H. Menzel, *J. Biotechnol.* **2012**, doi.org/10.1016/j.jbiotec.2012.06.036.